



This is a repository copy of *Limit analysis of reinforced embankments on soft soil*.

White Rose Research Online URL for this paper:
<http://eprints.whiterose.ac.uk/101359/>

Version: Accepted Version

Article:

Smith, C.C. orcid.org/0000-0002-0611-9227 and Tatari, A. (2016) Limit analysis of reinforced embankments on soft soil. *Geotextiles and Geomembranes*, 44 (4). pp. 504-514. ISSN 0266-1144

<https://doi.org/10.1016/j.geotexmem.2016.01.008>

Reuse

This article is distributed under the terms of the Creative Commons Attribution-NonCommercial-NoDerivs (CC BY-NC-ND) licence. This licence only allows you to download this work and share it with others as long as you credit the authors, but you can't change the article in any way or use it commercially. More information and the full terms of the licence here: <https://creativecommons.org/licenses/>

Takedown

If you consider content in White Rose Research Online to be in breach of UK law, please notify us by emailing eprints@whiterose.ac.uk including the URL of the record and the reason for the withdrawal request.



eprints@whiterose.ac.uk
<https://eprints.whiterose.ac.uk/>

Limit Analysis of Reinforced Embankments on Soft Soil

Colin C Smith^{a,*}, Alireza Tatari^a

^a*Department of Civil and Structural Engineering, The University of Sheffield, Mappin Street, Sheffield, S1 3JD, UK*

Abstract

Previous research into the stability of reinforced embankments founded on soft soil has presented limited studies based on a narrow range of assumed failure mechanisms. In this paper comprehensive parametric studies of reinforced and unreinforced embankments were conducted using the general purpose computational limit analysis approach Discontinuity Layout Optimization (DLO). Comparisons with previous Limit Equilibrium and FE results in the literature showed good agreement, with the DLO analysis generally able to determine more critical failure mechanisms. Simplified, summary design envelopes are presented that allow critical heights and reinforcement strengths to be rapidly determined based on soft soil strength and depth, and shows how the balance between soft soil strength and reinforcement strength combines to affect overall stability.

Keywords: Geosynthetics, discontinuity layout optimization, limit analysis, failure, reinforcement, safety factor.

1. Introduction

The use of a basal geosynthetic reinforcement for an embankment constructed on soft soils can significantly enhance stability and allow construction to heights substantially higher than could be achieved without reinforcement (Rowe and Soderman, 1987). Two common analysis methods used by geotechnical engineers to check the stability of embankments over soft soil are (i) conventional limit equilibrium such as Coulomb wedge or the method of slices and (ii) the finite element (FE) method. The general concept of the former method is to find the most critical slip surface with the lowest factor of safety. This may be defined as the shear strength of the soil divided by shear stress required for equilibrium, Duncan (1996).

*Corresponding author Tel: +44 114 2225717

Email addresses: c.c.smith@sheffield.ac.uk (Colin C Smith),
a.tatari@sheffield.ac.uk (Alireza Tatari)

12 Most limit equilibrium methods indirectly model the reinforcement as a sin-
13 gle representative force which acts at the intersection between the reinforcement
14 and the failure mechanism. The failure mechanism may be modelled as a slip-
15 circle using the method of slices (e.g. Rowe and Soderman (1985), Hird (1986),
16 Sabhahit et al. (1994)), or as a log-spiral (e.g. Leshchinsky (1987), Leshchinsky
17 and Smith (1989)) or using a translational mechanism (e.g. Jewell (1988)).

18 While limit equilibrium is simple and straightforward it makes an assumption
19 about the nature of the failure mechanism which can lead to inaccuracy. In
20 contrast FE methods can accurately model both working conditions and failure
21 modes, representing the reinforcement as a structural membrane with an axial
22 stiffness and negligible flexural rigidity. More recent work in the literature has
23 focused on this method *e.g.* Rowe and Soderman (1985); Rowe and Soderman
24 (1987); Duncan and Schaefer (1988); Hird and Kwok (1989); Hird et al. (1990);
25 Chai and Bergado (1993); Rowe and Hinchberger (1998); Rowe and Li (2005)
26 and Zhang et al. (2015). However, modelling the embankment problem by finite
27 elements typically requires significant time and is more complex with regard to
28 choosing the problem parameters in comparison with limit equilibrium methods
29 (Duncan, 1996).

30 Recently the advent of numerical direct methods has allowed the rapid solu-
31 tion of limit analysis problems in a fully general way. These provide a middle way
32 between the simplification in limit equilibrium analysis and the relative com-
33 plexity of the FE method. An elasto-plastic analysis typically requires many
34 increments in order to find the critical factor of safety in contrast to a compu-
35 tational limit analysis approach which can directly determine the collapse state
36 through optimization. One of the main advantages of limit analysis over FE
37 methods is it requires only two strength parameters for any material modelled:
38 the cohesion, c' or c_u , and the angle of shearing resistance, ϕ' , of the soil. Com-
39 putational limit analysis approaches have been recently used to analysis a range
40 of reinforced soil problems *e.g.* Leshchinsky et al. (2012), Clarke et al. (2013)
41 and Vahedifard et al. (2014). These papers utilise the Discontinuity Layout
42 Optimization method (Smith and Gilbert, 2007), which is adopted in this paper
43 to undertake a parametric study of embankment stability.

44 The aim of this paper is to illustrate how reinforced embankments can be
45 modelled in limit analysis; to investigate the range of failure modes that can
46 occur and to produce a series of non-dimensional design charts for different ge-
47 ometries of embankment which allows the necessary minimum embankment soil
48 strength and reinforcement strength required for stability to be determined in
49 terms of the embankment geometry, base soil strength, soil/geotextile interface
50 coefficient and surcharge. This provides a significantly more comprehensive set
51 of charts compared to previous works that have utilised Limit Equilibrium such
52 as Leshchinsky and Smith (1989), Duncan et al. (1987), Leshchinsky (1987) and
53 Hird (1986) without using an analysis which typically adopts only one mode of
54 failure.

55 2. Mechanics of reinforced embankments

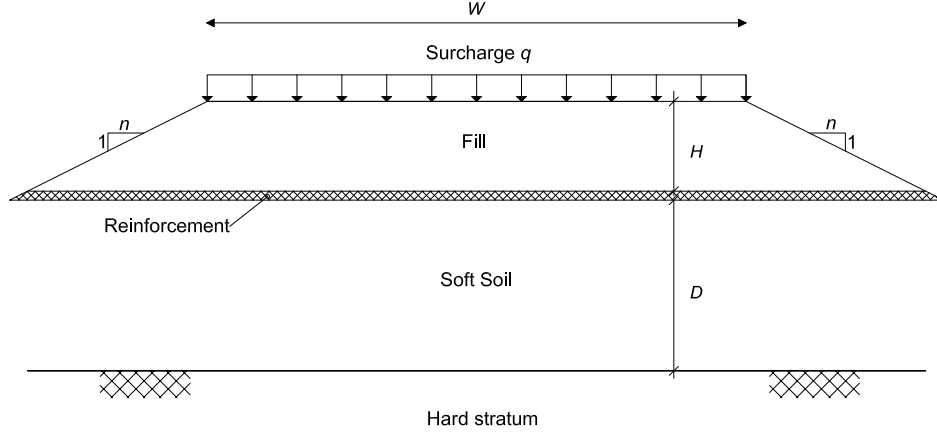


Figure 1: geometry of embankment model

56 Manceau et al. (2012) recommend three ULS states should be considered as
 57 follows: (i) deep-seated failure, (ii) lateral sliding (iii) extrusion. While deep
 58 seated failure requires an analysis such as method of slices or equivalent, the
 59 latter two mechanisms can be analysed relatively simply using limit equilibrium.
 60 Jewell (1988), presented simple analytical equations based on force equilibrium
 61 for the analysis of reinforced and unreinforced embankments of geometry de-
 62 picted in Figure 1 and described by the parameters listed in Table 1 (in the
 63 analysis $c' = 0$ was assumed). These provide useful equations for calibration
 64 and a conceptual model of two of the main mechanisms of collapse.

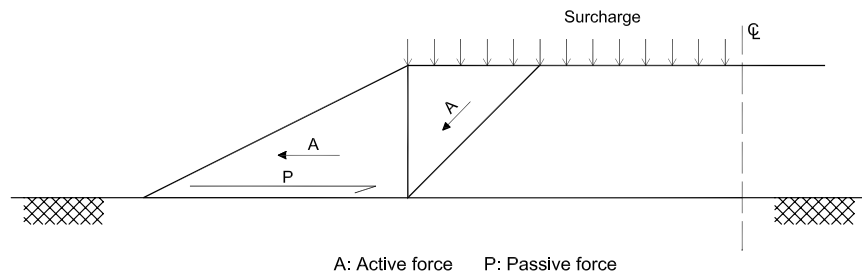
65 In Figure 2a, the reinforcement provides resistance against lateral failure
 66 of the embankment itself with friction on the upper reinforcement surface of
 67 $\alpha_s \tan \phi'$ where α_s is the reinforcement interface coefficient. Equilibrium analy-
 68 sis gives the following required side slope gradient n for stability:

$$n > \frac{K_a}{\alpha_s \tan \phi'} \left(1 + \frac{2q}{\gamma H}\right) \quad (1)$$

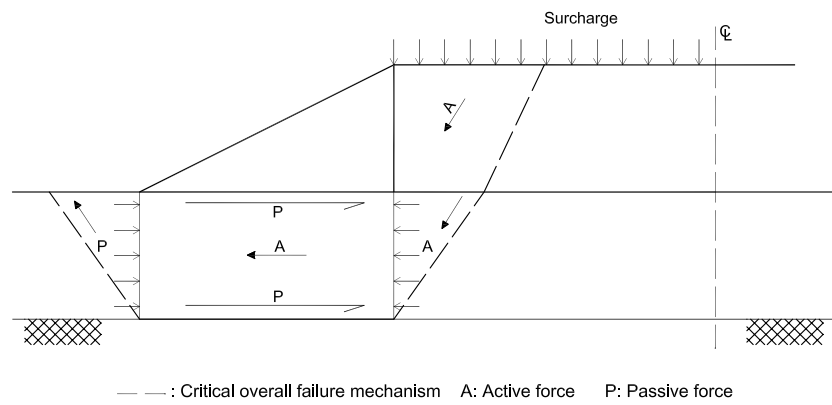
69 where the design value of active earth pressure coefficient, $K_a = \frac{1 - \sin \phi}{1 + \sin \phi}$.

70 In Figure 2b the reinforcement provides shear resistance against lateral
 71 squeezing of the soft soil beneath the embankment. Equilibrium analysis of
 72 the deep failure mechanism gives the factor of safety F_s on the soft soil strength
 73 as follows:

$$F_s = \frac{c_u}{q + \gamma H} \left(4 + (1 + \alpha_c) \frac{nH}{D}\right) \quad (2)$$



(a) Lateral sliding

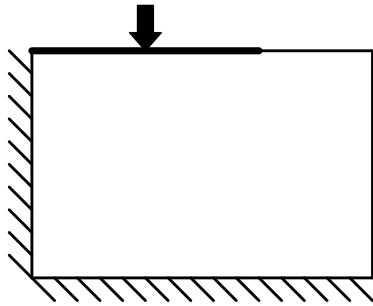


(b) Extrusion

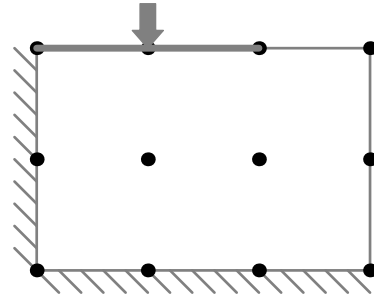
Figure 2: The mechanism of failure of embankment over soft soil (after Jewell, 1996)

Table 1: Reinforced embankment analysis parameters

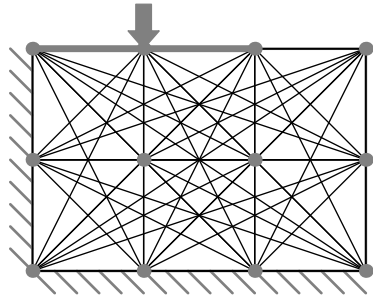
Symbol	Definition
c'	cohesion of the soil of embankment fill
ϕ'	friction angle of soil of embankment fill
γ	unit weight of soil of embankment fill
c_u	shear strength of soft soil
R	rupture strength of reinforcement per unit width
H	height of embankment
W	width of top of embankment
D	thickness of soft soil
q	surcharge
n	side slope gradient ($nH : 1V$)
α_c	interface coefficient between reinforcement and soft soil
α_s	interface coefficient between reinforcement and embankment fill



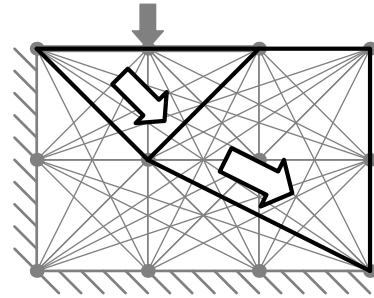
(a) Initial problem (rigid load applied to block of soil close to a vertical cut).



(b) Discretize domain area using nodes.



(c) Interconnect every node to every other node with a potential discontinuity.



(d) Identify critical layout of discontinuities at collapse using optimization.

Figure 3: Stages in DLO solution procedure (after Gilbert et al. (2010)).

74 The minimum force R within the reinforcement required to provide the sta-
 75 bility for the failure mechanism in Figure 2b is given by equation 3:

$$R = \gamma H^2 \left(\frac{\alpha n D}{4D + (1 + \alpha)nH} + \frac{K_a}{2} \right) \quad (3)$$

76 Jewell also presented the following equation for checking the stability of an
 77 unreinforced embankment (the failure mechanism is not present here):

$$F_s = \frac{c_u}{\gamma H} \left(\frac{8D + 2nH}{2D + K_a} \right) \quad (4)$$

78 Such limit equilibrium equations have the value of simplicity and clarity but
 79 it is not necessarily clear whether these are conservative or non-conservative in
 80 all cases.

81 3. Discontinuity layout optimisation (DLO)

82 3.1. Geotechnical analysis

83 Discontinuity layout optimization is a computational limit analysis method
 84 which is able to identify the critical failure mechanism and collapse load for any
 85 geotechnical stability problem. Examples of this analysis approach applied to
 86 soil only problems (with no reinforcement) may be found in [Smith and Gilbert](#)
 87 [\(2007, 2013\)](#) and [Leshchinsky \(2015\)](#). Figure 3 illustrates the stages in the
 88 DLO procedure for finding the layout of sliplines that form the critical collapse
 89 mechanism (after [Gilbert et al. 2010](#)). The accuracy of the method depends on
 90 the number n nodes employed which allow the critical mechanism to be selected
 91 out of a set of $n(n - 1)/2$ potential sliplines. Using the principles of duality,
 92 the DLO formulation may be presented in either a kinematic energy form or an
 93 equilibrium and yield form.

94 3.2. Modelling reinforcement in DLO

95 Reinforcement is modelled as a one dimensional element similar to that de-
 96 scribed by [Clarke et al. \(2013\)](#). This element is able to model failure in bending,
 97 tensile rupture and compressive failure controlled by parameters M_p , R , and C
 98 respectively, where M_p is the plastic moment of resistance and C is the com-
 99 pressive strength of the reinforcement. The element described by [Clarke et al.](#)
 100 [\(2013\)](#) was designed also to allow the modeling of soil nails and so had the ad-
 101 ditional ability to allow soil to ‘flow around’ the element controlled by a lateral
 102 and pullout resistance. In this paper these properties were not required and
 103 these resistances were set to ∞ .

104 Each engineered element has three parallel components (as shown in Fig-
 105 ure 4) which comprise: an upper boundary interface, the reinforcement itself
 106 and a lower boundary interface. For the purposes of modelling geotextile rein-
 107 forcement M_p is set to zero to allow free flexure, C is set to zero and the upper
 108 and lower boundaries are modelled with Mohr-Coulomb materials with strength
 109 $\alpha_s \tan \phi'$ and $\alpha_c c_u$ respectively.

110 In the equilibrium formulation of DLO, for each discrete element i of the
 111 reinforcement, variables are assigned to represent the shear stress $\tau_{u,i}, \tau_{l,i}$, on
 112 the upper and lower faces respectively, and the tensile force T_i and bending
 113 moment M_i in the reinforcement. The set of τ_u, τ_l, M, T are found that give
 114 the maximum load on the system that does not violate the following constraints:

- 115 1. $\tau_l \leq \alpha_c c_u$
- 116 2. $\tau_u \leq \alpha_s (c' + \sigma'_n \tan \phi')$
- 117 3. $C \leq T \leq R$
- 118 4. $M \leq M_p$

119 where σ'_n is the effective normal stress acting on the reinforcement.

120 It is noted that even if $M_p = R = C = 0$, the modelled reinforcement
 121 will still affect the mechanics of the system in that shear displacements are not
 122 permitted directly through the reinforcement element. However this can be
 123 represented via element rotations. With sufficiently small segments the same
 124 effect is achieved. Use of a higher nodal density along the reinforcement can
 125 therefore be beneficial in some cases.

126 Note that in a limit analysis formulation such as DLO, yield or rupture of the
 127 reinforcement does not lead to breakage or fracture but to unrestricted ductile
 128 elongation that still allows transmission of tensile forces along the length of the
 129 reinforcement.

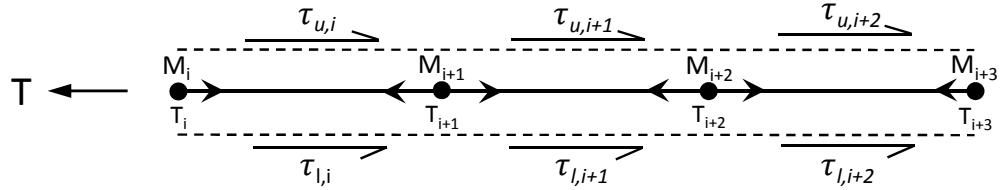


Figure 4: Modelling flexible reinforcement in DLO for segment or node i , τ_u : upper boundary soil/reinforcement interface stress (kPa), τ_l : lower boundary soil/reinforcement interface stress (kPa), T : tensile force in reinforcement (kN, per m width), M : bending moment in reinforcement (kN, per m width).

130 4. Embankment modelling

131 4.1. Numerical model

132 Analysis was carried out using the implementation of DLO within the soft-
 133 ware LimitState:GEO Version 3.2a (LimitState, 2014). In the model, the bound-
 134 ary nodal spacing was set to be half that within the internal solid bodies as is
 135 recommended (LimitState, 2014). A series of internal vertical boundaries were
 136 also modelled within the embankment to allow ‘bending’ (or ‘snapping’) failure
 137 of the embankment. A simple example of this is shown in Figure 5d. Selected

138 models across the parameter space were evaluated using nodal spacings on a
139 square grid of $H/1$ to $H/10$. Typical results are shown in Appendix A. Based
140 on these an accuracy of 1-2% in terms of the factor of safety on soil strength
141 would be achieved with a nodal spacing of $H/5$. This spacing was selected as a
142 compromise between accuracy and speed.

143 *4.2. Failure mechanisms*

144 Four distinct mechanisms of failure were generated by the DLO analysis and
145 are shown in Figure 5. These mechanisms can be described as follows:

- 146 (a) Lateral sliding failure (surface failure).
- 147 (b) Deep seated global failure.
- 148 (c) Lower layer failure (squeezing/extrusion failure) with sinking.
- 149 (d) Lower layer failure (squeezing/extrusion failure) with ‘snapping’.

150 For a high strength lower stratum, failure is in the shoulders of the embank-
151 ment only (Figure 5a). For low strength reinforcement the dominant failure
152 mechanism is a deep seated global failure accompanied by yield of the reinforce-
153 ment (Figure 5b). In this type of failure, significant shearing happens in the
154 main body and side slopes of the embankment. For high strength reinforcement
155 significant ‘squeezing’ deformation is primarily seen in the lower stratum. The
156 embankment itself either undergoes very localised shearing and vertical ‘sink-
157 ing’ translation (Figure 5c) or rotational ‘snapping’ (Figure 5d). The latter
158 mechanism is more likely to occur and need not involve any significant defor-
159 mation/yielding of the reinforcement which simply rotates. To the authors’
160 knowledge, the latter type of failure has not been previously examined in the
161 literature.

162 *4.3. Verification*

163 *4.3.1. Translational failure mechanisms*

164 To permit direct comparison between the analytical solutions of Jewell (1988)
165 and the DLO method for the analysis of surface failure (equation 1 and figure
166 2a), a simplified constrained model was first set up in DLO, setting the bound-
167 aries of the model to coincide exactly with the mechanism geometry used by
168 Jewell. The relevant soil properties were applied to these boundaries while the
169 solid bodies between the boundaries were assigned a rigid material of the same
170 unit weight as the soil. This ensures failure can only occur along the pre-defined
171 boundary lines, thus forcing the mechanisms to match those of Jewell’s. The
172 results, given in Figure 6, show, as expected, that the constrained DLO analy-
173 sis exactly matches the analytical solution (which can be regarded as an upper
174 bound analysis) while the unconstrained DLO analysis, results also given in
175 Figure 6, give more critical results.

176 Figure 7 illustrates the comparison between the results of DLO and equations
177 2 and 4 for deep seated failure of reinforced and unreinforced embankments
178 respectively. The results of analyses show a good match. However the DLO
179 results are not consistently more critical as might be expected. This can be

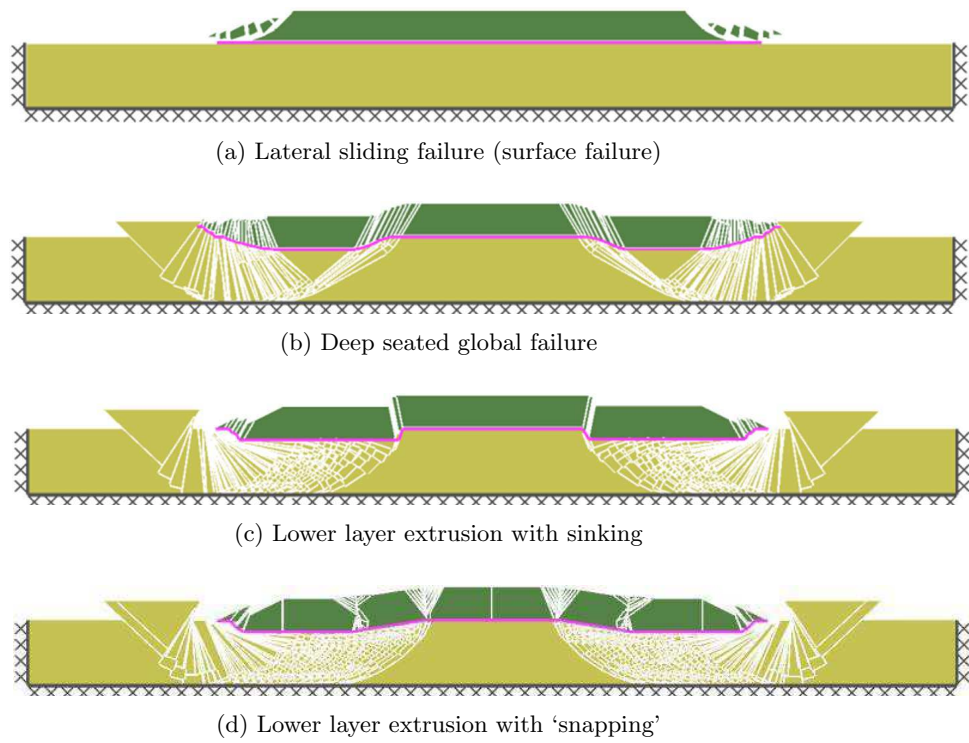


Figure 5: Failure mechanisms of embankment over soft soil (exaggerated)

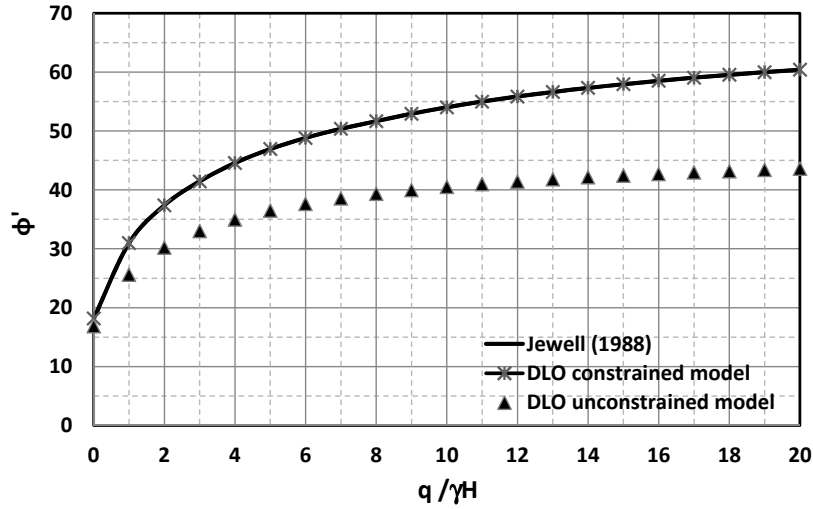


Figure 6: Plot of ϕ' required for factor of safety of 1.0 against $q/\gamma H$ for Jewell's analytical method (1988) and the current approach ($n = 2$ and $\alpha_s = 0.8$).

180 attributed to the form of the analytical equations which are based on limit
 181 equilibrium rather than limit analysis and, while probably not adopting an
 182 optimal mechanism, do neglect soil strength in various parts of the system.

183 4.3.2. Rotational mechanisms

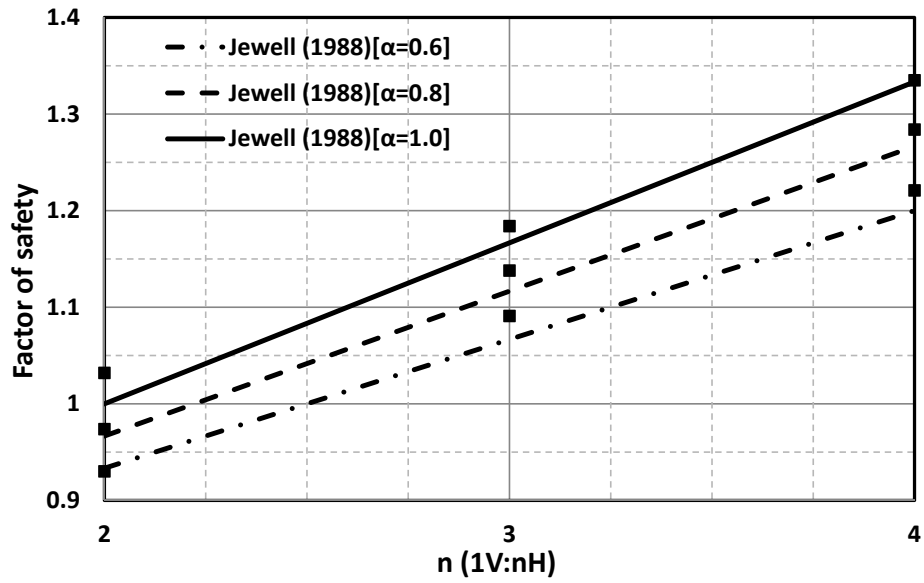
184 Leshchinsky and Smith (1989) used an upper bound log-spiral rotational
 185 analysis for checking the factor of safety of an unreinforced embankment con-
 186 structed on soft clay. The results were expressed in terms of a stability number:

$$N_m = \frac{1}{\gamma H} \frac{c_u}{F_s} \quad (5)$$

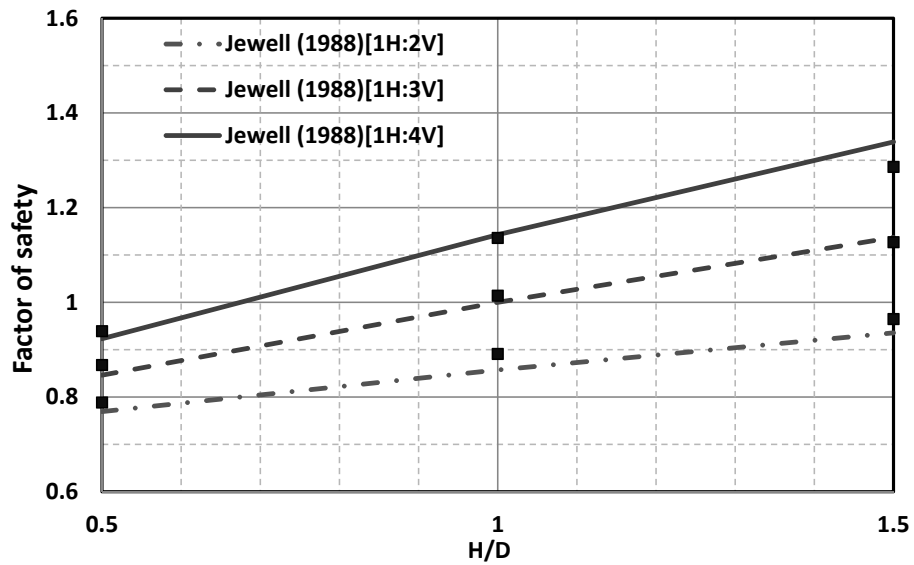
187 where F_s is the required factor of safety.

188 The comparison of DLO analyses with those of Leshchinsky and Smith given
 189 in Figure 8 show close agreement, with DLO generally able to identify a more
 190 critical case as would be expected, since it is not restricted to one single failure
 191 mode. However the specific mechanism utilised Leshchinsky and Smith outper-
 192 formed the DLO analysis marginally in two of the cases considered. This is not
 193 unexpected for circumstances where their mechanism closely matches the exact
 194 solution.

195 Figure 9 compares results of the DLO and the log-spiral limit analysis of
 196 Leshchinsky (1987) for a stability of embankment over soft soil. Leshchinsky
 197 (1987) checked bearing failure and deep seated failure. The results of the study
 198 showed that DLO was able to identify a more critical failure mechanism for all
 199 the above modes and in addition for surface lateral sliding.



(a) Reinforced embankment over soft soil



(b) Unreinforced embankment over soft soil

Figure 7: Plot of factor of safety against side slope gradient (n) for Jewell's analytical method (1988) and the current method (square markers) using parameters $c_u = 15\text{kPa}$, $\gamma = 18\text{kN/m}^3$, $\phi' = 30^\circ$.

200 Hird (1986) produced a series of non-dimensional charts for cohesive and
201 cohesionless reinforced embankments over soft soil using the limit equilibrium
202 method of slices in which the reinforcement was modelled by applying a hori-
203 zontal force to the sliding mass of soil. Figure 10 again shows good agreement,
204 though since the work by Hird was based on Limit Equilibrium it is not possible
205 to comment specifically on the relative magnitudes.

206 4.3.3. FE analysis

207 Rowe and Li (1999) and Rowe and Soderman (1987) investigated reinforced
208 embankment problems by using finite element analysis. They investigated the
209 required tensile stiffness of reinforcement (J : kN/m) for a given embankment
210 height to achieve a factor of safety of one, and reported the maximum strain
211 (ϵ_f) in the reinforcement at that point. A Limit Analysis method such as DLO
212 cannot model elastic stiffness. Therefore to enable comparisons, the equivalent
213 rupture strength R is calculated from the following equation:

$$R = J\epsilon_f \quad (6)$$

214 This limits the mobilised tensile stress in the reinforcement to the maximum
215 value modelled in the FE analysis. However while in the FE model, this value
216 represents the peak mobilised strength, possibly at one location only, in the DLO
217 LA model, the mobilised strength is free to be distributed along the length of
218 the reinforcement.

219 The model parameters investigated are given in Table 2. Figure 11 shows the
220 corresponding maximum height H of the embankment for a variety of reinforce-
221 ment rupture strengths. The results of the study shows that the FE method
222 generally found more critical results (i.e. higher required rupture strengths) in
223 comparison with DLO. This is attributed to the DLO model being able to redi-
224 stribute the yield stress within the reinforcement, while the corresponding value
225 in the FE model may only be a single peak value. However it is observed that
226 this does not fully agree with the results of Tandjiria et al. (2002) who modelled
227 the same scenarios using limit equilibrium and achieved closely similar results
228 to the FE models with a range of different distributions of mobilised strength
229 along the length of the reinforcement.

230 In summary the results show generally very good agreement with previous
231 work, validating the DLO approach but also indicates that DLO is able to find
232 more critical mechanisms in most cases.

233 5. Parametric study

234 5.1. Non-dimensional charts

235 The parametric study employed in this study investigated the geometry de-
236 picted in Figure 1 and the parameters given in Table 1. For a horizontal stratum
237 of soil, the unit weight has no effect in undrained collapse, therefore the weight
238 of the soft soil need not be considered. To efficiently cover a wide range of pos-
239 sible parameters, the study was conducted using the following 8 independent

Table 2: FE model comparison. Reinforced embankment analysis parameters. The undrained strength c_u varies linearly with depth z below the soft soil surface.

Parameter	Embankment 1 (Rowe and Soderman, 1987)	Embankment 2 (Rowe and Li, 1999)
W	30m	27m
n	2	2
ϕ'	32°	37°
γ	20 kN/m ³	20 kN/m ³
c_u ($z=0$ m)	10kN/m ²	5.0kN/m ²
c_u ($z=15$ m)	40kN/m ²	27.5kN/m ²
D	15m	15m
α_c	1.0	1.0
α_s	1.0	1.0

240 non-dimensional groups:

241

242

$$c'/\gamma H, c_u/\gamma H, R/\gamma H^2, q/\gamma H, H/D, n, \alpha \text{ and } \phi'$$

243

244

245

246

247

248

249

250

251

252

H was chosen as a normalising parameter for the first four groups since an increase in height of the embankment is expected to have the most significant effect on the stability. It was assumed that the embankment was sufficiently wide to avoid the collapse mechanism involving the centre. Based on the numerical model results, minimum values of W/D of approximately $4 + 2H/D$ are required for this assumption to hold true for most typical parameter sets. A comprehensive set of 72 charts were generated and are available in Electronic Annex 1 in the online version of this article. Different charts are presented for different values of:

253

- surcharge $q/\gamma H$ (0.0, 0.1),

254

- Interface coefficient α (0.6, 0.8, 1.0),

255

256

- Ratio of height of embankment and thickness of soft soil H/D (0.5, 1.0, 1.5),

257

- Angle of side slope 1V:nH (2, 3, 4),

258

- Low or high rupture strength of reinforcement $R/\gamma H^2$ (0.1, 1.0).

259

260

261

An example non-dimensional chart is presented in Figure 12 in terms of ϕ' vs $c_u/\gamma H$ for a range of values of $c'/\gamma H$. All graphs show the same qualitative pattern.

262

263

According to FHWA-NHI-00-043 (2001) the normal interface factor for geogrid and geotextiles varies between 0.6 and 0.8 respectively. In most design

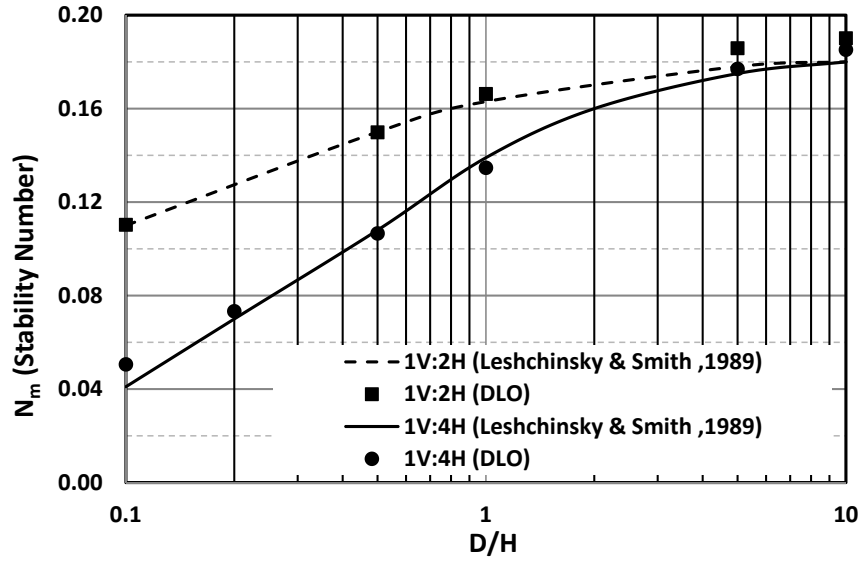


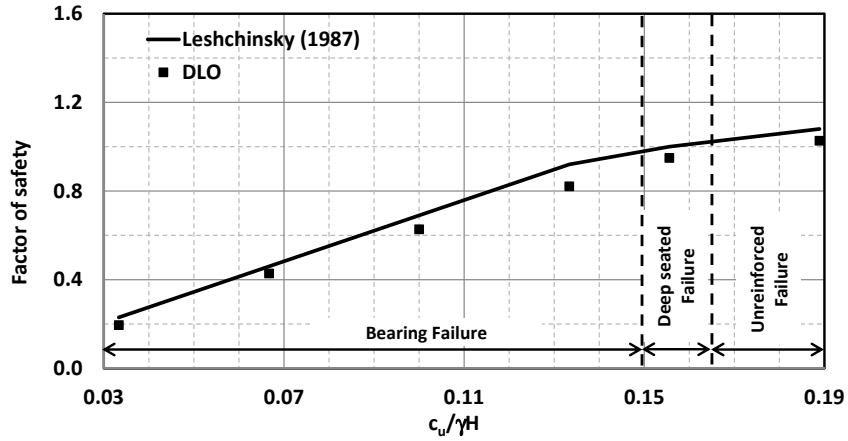
Figure 8: Comparison the result of DLO & Leshchinsky and Smith (1989) for an unreinforced embankment over soft soil. ($\phi' = 30^\circ$)

264 guidelines and work examples, the interface coefficient for both top and bottom
 265 surfaces of the reinforcement is selected to be the same which has been done
 266 in this paper. Therefore the stated three interface coefficient values were model-
 267 elled: 0.6, 0.8 and 1.0. It was necessary to model this only for the high rupture
 268 strength reinforcement because the dominant failure mechanism for weak rein-
 269 forcement is global failure which is insignificantly affected by the shear resistance
 270 generated between the soil and geotextile. These parameters cover most typical
 271 embankments which are constructed over soft soil. Due to the symmetry of the
 272 model, only half of the cross-section was analysed with a symmetry boundary
 273 at one edge.

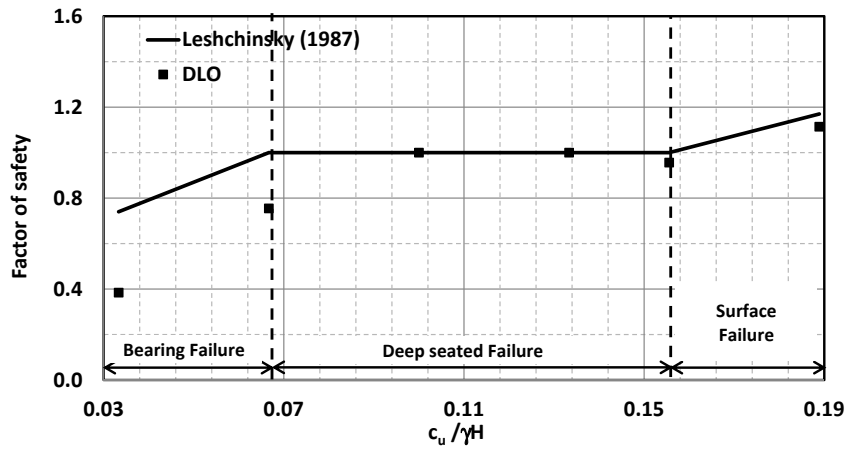
274 The maximum stable slope angle of a granular material is fundamentally
 275 related to the friction angle of the soil. Therefore, an embankment with zero
 276 cohesion and angle of friction less than the side slope angle is unstable. In this
 277 study, in order to extend the non dimensional graphs in this area, a small value
 278 of c' (equal to 0.1kPa) was set throughout the soil body to avoid local slope
 279 instability failure. Where this is done, it is indicated by a dashed line. Finally,
 280 for the design charts for the embankment with surcharge, there is no stable
 281 solution for a zero value of c' hence these are omitted from the charts.

282 5.2. Reinforcement strength

283 Two values of $R/\gamma H^2$ were employed in the generic parametric study, 0.1
 284 and 1.0. This was intended to cover a broad range from very weak reinforcement
 285 (0.1) and strong reinforcement (1.0). To investigate the effect of reinforcement



(a) $H/D=0.1$



(b) $H/D=1.0$

Figure 9: Comparison of DLO and Leshchinsky (1987) for an embankment with slope 1V:2H over soft soil for $\phi'=30^\circ$. The factor of safety was on the shear strength of the soil. The mechanism description is based on the DLO analysis.

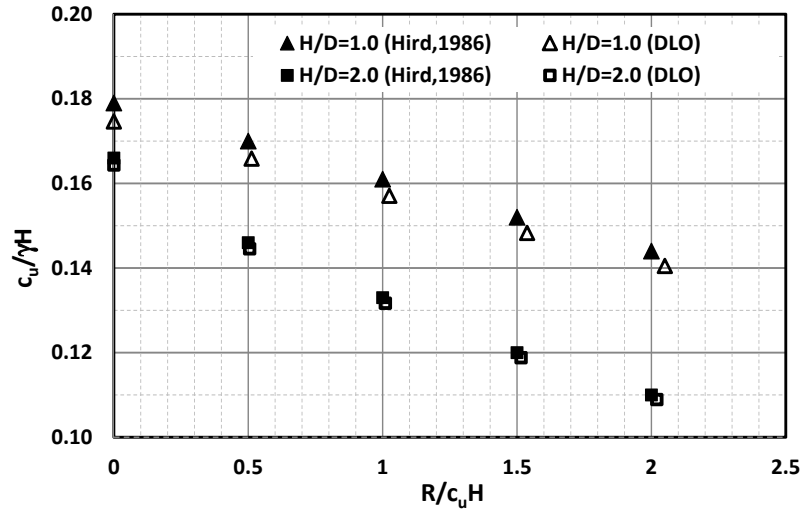


Figure 10: Plot of normalised undrained shear strength of soft soil required for stability against normalised reinforcement resistance for current method and Hird (1986). ($1V : 1.75H$, $H=5\text{m}$, $\gamma=18\text{kN/m}^3$, $\phi'=30^\circ$)

286 on stability, specific studies were also undertaken over a broad range of values of
 287 $R/\gamma H^2$. Figures 13a and b show how $c_u/\gamma H$ varies with reinforcement strength
 288 $R/\gamma H^2$ for a specific parameter set ($H/D = 0.5$, $1V:2H$, $c' = 0$ and $\alpha = 0.8$).
 289 It can be seen that for the no surcharge case, the solutions are independent of
 290 $R/\gamma H^2 > 1.0$ (this value will be defined as the limiting value $R_L/\gamma H^2$, at which
 291 the embankment will be said to be fully reinforced), and that there is a generally
 292 linear relationship between the parameters between $R/\gamma H^2=0$ to 0.7 . Therefore
 293 if it is necessary to interpolate for R , a conservative approximation is to linearly
 294 interpolate between the values of $R = 0$ to R_L . An example interpolation is
 295 indicated in Figure 13b. In order to ensure conservative results, it can be seen
 296 that there will be a small error in the interpolation which is maximum between
 297 around $0.5R_L$ to $0.6R_L$. This maximum error is around 8% in c_u or around 20%
 298 in R . Further examples of the bilinear fit for a number of different parameter
 299 sets are reported in Electronic Annex 1 in the online version of this article and
 300 show similar behaviour.

301 Furthermore it can be seen that $R/\gamma H^2$ is very sensitive to changes in $c_u/\gamma H$,
 302 for values of $R < R_L$. Ideally the reinforcement should be designed from the
 303 horizontal portion of the curves (i.e. using R_L) and in design it would be
 304 preferable to apply a (partial) factor of safety to c_u rather than to R , or to
 305 both.

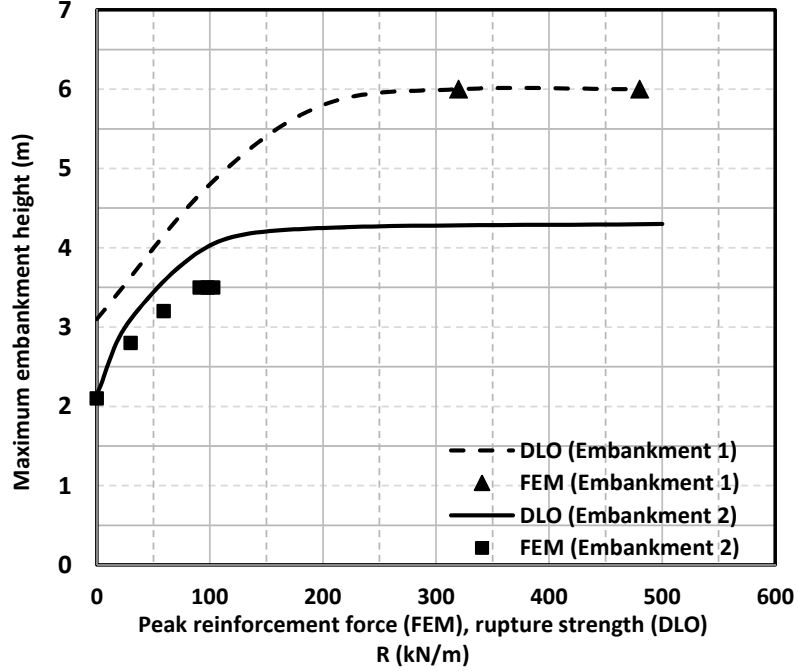


Figure 11: Comparison of the maximum height H of embankment versus reinforcement rupture strength R for current method, and peak reinforcement force for Rowe and Soderman, 1987 (Embankment 1) and Rowe and Li, 1999 (Embankment 2). Model parameters are given in Table 2.

306 5.3. Simplified design envelopes

307 It can be seen from the preceding graphs that the design region between
 308 fully stable or fully unstable embankments is relatively small in terms of the
 309 values of $c_u/\gamma H$. For example in Figure 13(b), independent of the value of
 310 $R/\gamma H^2$, and assuming that $\phi' = 30^\circ$ always, the system will always be stable
 311 for $c_u/\gamma H > 0.176$ and always unstable for $c_u/\gamma H < 0.125$. Variants in the
 312 value of ϕ' would change these values only by around 10% for failure modes
 313 where failure in the soft soil layer dominates. Other graphs e.g. Figure 12 show
 314 that additionally $c'/\gamma H$ also has a small effect (<10% on the value of $c_u/\gamma H$).

315 It is thus possible to plot a simplified design envelope of $c_u/\gamma D$ vs H/D
 316 for $\alpha = 0.8$, shown in Figure 14(a) for $\phi' = 30^\circ$ and $c'/\gamma H = 0.0$ and Figure
 317 14(b) for $\phi' = 50^\circ$ and $c'/\gamma H = 0.1$. Two curves are given. Above the upper
 318 value the system is always stable (this corresponds to $R = 0$). Below the lower
 319 limit, it is generally always unstable (though minor gains may be made with
 320 stronger fill) and this corresponds to $R = R_L$. Values of $R_L/\gamma D^2$ are given
 321 on the same graph. In between the values the more detailed design charts

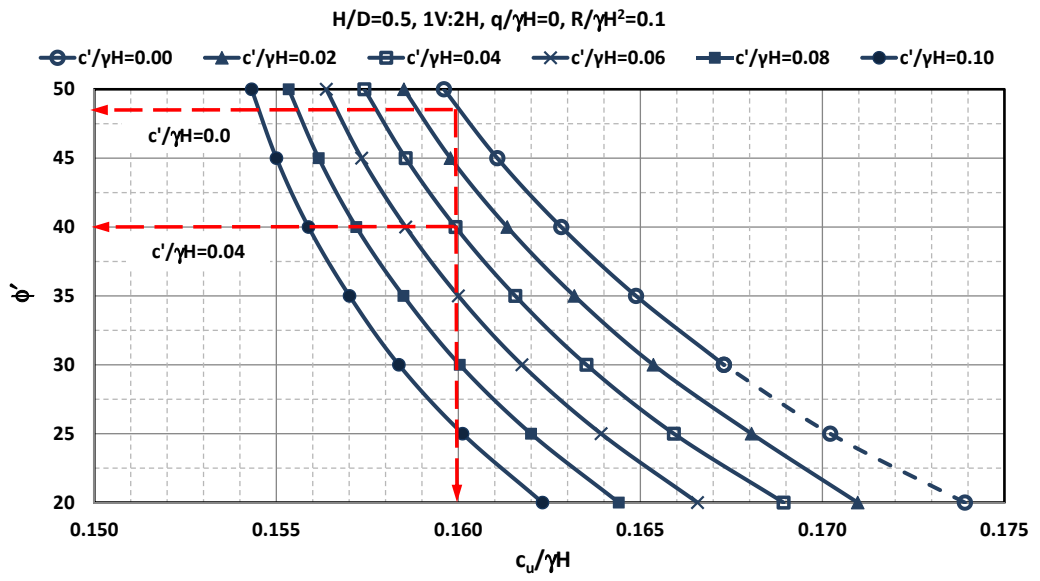
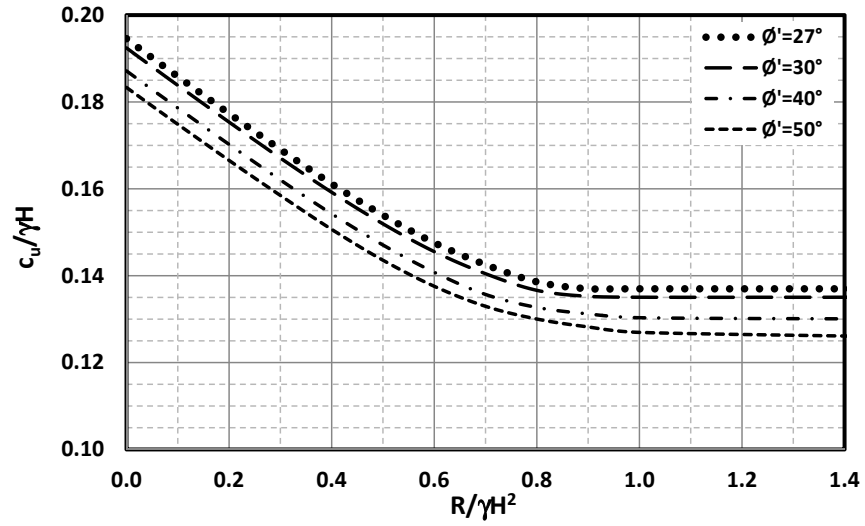
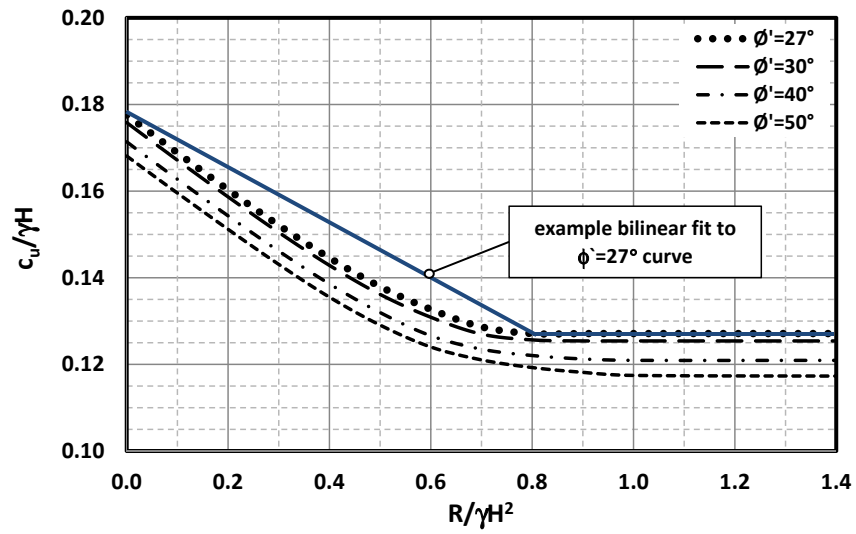


Figure 12: Value of ϕ' required for stability vs $c_u/\gamma H$ for $H/D = 0.5$, $n = 2$, $q = 0$ and $R/\gamma H^2 = 0.1$. This illustrates the type of graph generated from the parametric study discussed in Section 5. The long-dashed lines illustrate the design example presented in Section 6. A further 72 graphs are available in Electronic Annex 1 in the online version of this article.



(a) With surcharge, $q/\gamma H = 0.1$



(b) Without surcharge

Figure 13: Required undrained shear strength for stability plotted against reinforcement strength ($H/D = 0.5$, $1V:2H$, $c' = 0$ and $\alpha = 0.8$).

322 must be used, or, as discussed previously, a linear interpolation can be used to
 323 provide a good estimate of R . Note that for these graphs the values of c_u and
 324 R_L have been normalised using D rather than H since this is expected to be
 325 an independent variable. Overall it can be seen that the use of reinforcement
 326 allows an embankment of a given size to be constructed on soft soil of around
 327 50-100% the strength of that on which an unreinforced embankment could be
 328 constructed, depending on the value of H/D . It can also be seen that stronger
 329 fill has a marginal effect on the performance of a reinforced embankment, but a
 330 more significant effect on the stability of an unreinforced embankment.

331 Figure 14(b) also indicates that, for this example, an almost unlimited height
 332 of a fully reinforced embankment is possible for $c_u/\gamma D > \sim 0.16$ which may seem
 333 paradoxical, however this arises because the mechanism of failure is squeezing
 334 of the (relatively thin) confined soft soil layer which occurs over a width that
 335 extends beyond the embankment crest. Since the side slope width increases
 336 in tandem with the height, the bearing resistance in the soft soil layer also
 337 increases. It is noted that the reinforcement strength must also increase signif-
 338 icantly with the height.

339 Finally Figure 15 shows that the limit equilibrium approach recommended
 340 by Jewell (1988), for extrusion only, provides a generally good fit to the data
 341 and is only slightly conservative compared with the current results for a fully
 342 reinforced embankment. The values it recommends involve an approximately
 343 20% higher value of $c_u/\gamma D$ for a given H/D , but an approximately 10% smaller
 344 value of $R_L/\gamma D^2$. In combination this should still give a stable state but is
 345 slightly overconservative. To confirm this the interpolation method discussed in
 346 Section 5.2 was used on the Jewell value of $c_u/\gamma D$ to predict the corresponding
 347 required reinforcement strength $R/\gamma D^2$ using the current method. It can be
 348 seen that a value lower than the Jewell value of $R/\gamma D^2$ is predicted.

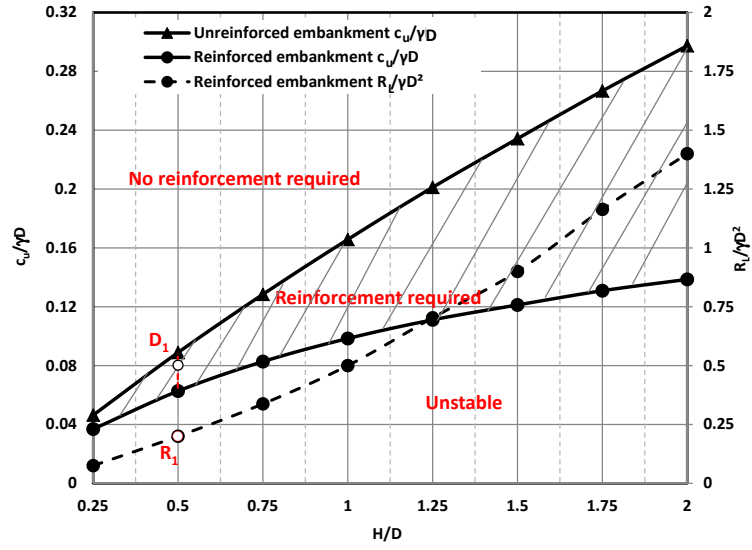
349 However, it is suggested that it would be preferable to design with the value
 350 of R_L to avoid the sensitivity to c_u discussed previously. It would also be
 351 expected that the extrusion equations would become less valid for values of
 352 $H/D < 0.25$, as a deep seated failure mode becomes more dominant.

353 6. Design example

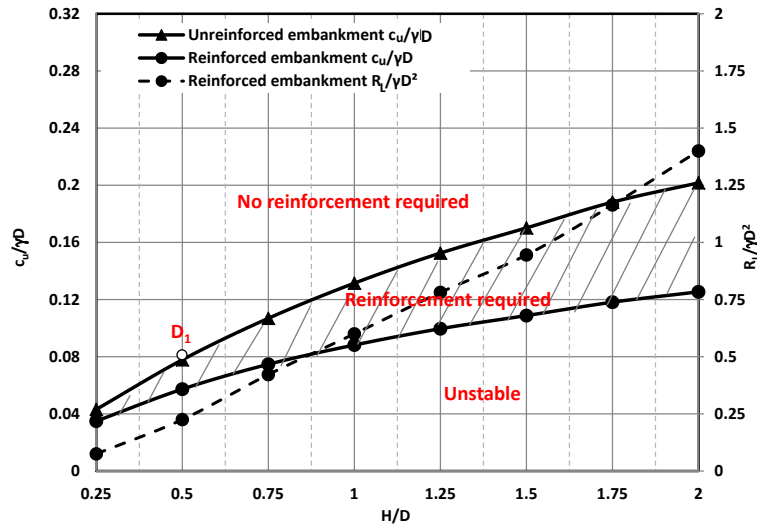
354 Consider an embankment of 5m height and side slope $1H : 2V$ constructed
 355 from a coarse grained material of unit weight 17.5kN/m^3 overlying 10m of soft
 356 soil of uniform shear strength $c_u = 14\text{kPa}$ as shown in Figure 16. The re-
 357 quired soil strength for the embankment fill when using a low rupture strength
 358 reinforcement (with $\alpha = 0.8$) without surcharge is determined as follows.

359 From Figure 14(a), it can be seen that design point D_1 plots at $(H/D,$
 360 $c_u/\gamma D) = (0.5, 0.08)$ and that this lies between the maximum and minimum
 361 curves. In order to estimate the required reinforcement strength, the value
 362 $R_L/\gamma D^2 = 0.20$ can be read off the same graph (point R_1) for $H/D = 0.5$. This
 363 reinforcement strength is sufficient to support an embankment on a soil with
 364 $c_u/\gamma D = 0.063$. It is then possible to interpolate as follows:

365 Taking $c_{u,min}/\gamma D = 0.063$, $c_{u,max}/\gamma D = 0.089$, and $R_L/\gamma D^2 = 0.20$.



(a) $\phi' = 30^\circ, c' = 0$



(b) $\phi' = 50^\circ, \frac{c'}{\gamma H} = 0.1$

Figure 14: Simplified design domains ($\alpha = 0.8, q = 0$ and $n = 2$). The reinforced embankment case uses reinforcement with rupture strength R_L the value of which is given in the same plot. The shaded zone is the design domain where reinforcement is required. Below this zone stability is not possible with a single layer of reinforcement.

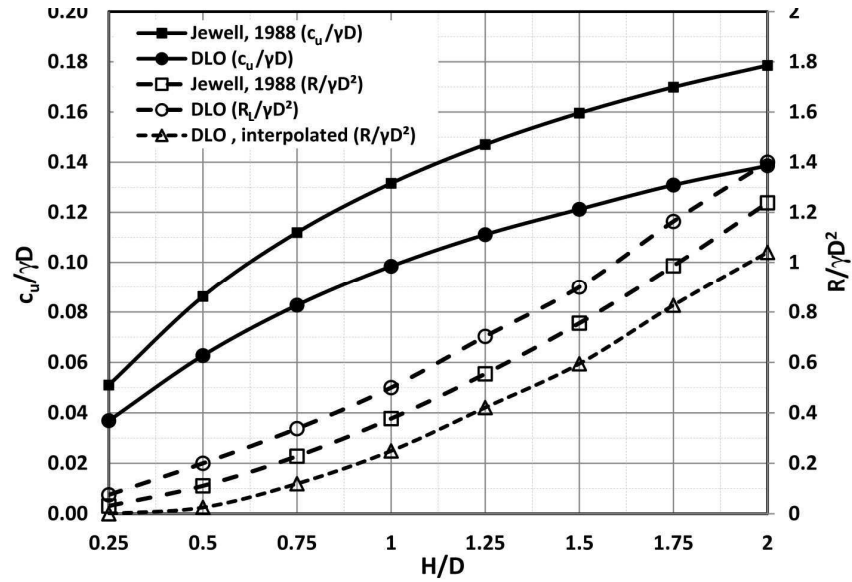


Figure 15: Comparison of results from the current method and Jewell (1988), equations 2 and 3, for determining the required shear strength of soft soil and rupture strength of reinforcement for stability $\phi' = 30^\circ$, $c' = 0$, $\alpha = 0.8$, $q = 0$ and $n = 2$). The ‘interpolated’ line shows the predicted required value of $R/\gamma D^2$ using the current method based on the value of c_u specified by the method of Jewell.

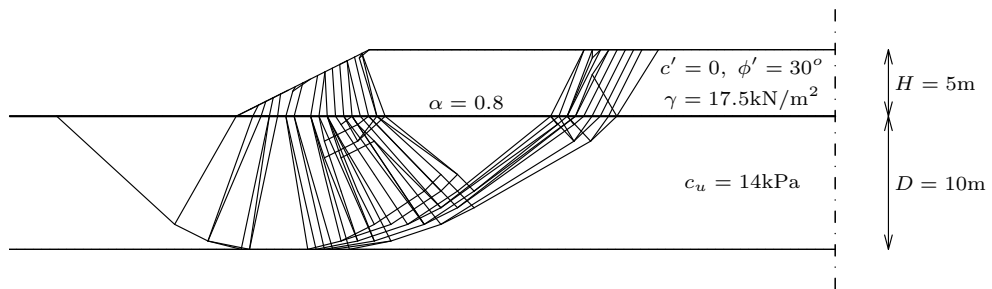


Figure 16: Design example geometry and failure mechanism associated with the determined geotextile rupture strength $R = 121$ kN/m.

$$\frac{R}{\gamma D^2} = \frac{R_L}{\gamma D^2} \frac{c_{u,max} - c_u}{c_{u,max} - c_{u,min}} = 0.20 \frac{0.089 - 0.08}{0.089 - 0.063} = 0.069 \quad (7)$$

366 Hence the required reinforcement tensile strength R is 121 kN/m. This
 367 result is valid for embankment fill of $\phi' = 30^\circ$ and $c' = 0$ and will be slightly
 368 overconservative due to the linear interpolation approximation. For a stronger
 369 fill of $\phi' = 50^\circ$ and $c' = 0.1\gamma H = 8.8$ kN/m², Figure 14(b) indicates that no
 370 reinforcement is required.

371 As noted before R has a significant degree of sensitivity to $c_u/\gamma H$, e.g. a
 372 reduction in c_u of 10% can lead to a change in R of 60%. However a reduction
 373 in c_u of 15% will lead to a situation that cannot be stabilised by reinforcement.
 374 For a more detailed study, the case of $R/\gamma H^2 = 0.1$ can be investigated using
 375 the charts presented in Electronic Annex 1 in the online version of this article.
 376 The graph therefore corresponds to a model where the reinforcement rupture
 377 strength is a low value of $R = 44$ kN/m. In this case failure is typically by
 378 reinforcement rupture, combined with soil failure.

379 First the relevant chart is chosen (shown also in Figure 12) based on the
 380 values of $H/D = 0.5$, slope $1H : 2V$, and $q/\gamma H = 0$. Having selected the
 381 graph, the x -axis can be read off using $c_u/\gamma H = 0.16$. A family of curves then
 382 allows different combinations of c' and ϕ' to be selected such as ($c' = 0, \phi' = 48^\circ$)
 383 or ($c'/\gamma H = 0.04$, ie $c' = 3.5$ kPa, $\phi' = 40^\circ$) which is the required shear strength
 384 of the embankment soil for a factor of safety of 1.0. This is consistent with the
 385 previous result that indicated that reinforcement was not necessary for $\phi' = 50^\circ$.
 386 If higher factors of safety are required then these can be applied as appropriate
 387 to the parameters.

388 7. Discussion

389 The validation studies indicate that the factor of safety computed with the
 390 DLO method is typically lower than the conventional limit analysis and limit
 391 equilibrium methods. This is due to the critical failure mechanism not being
 392 pre-defined. However the DLO results were slightly above those given by the
 393 FE analyses of Rowe and Li (1999) and Rowe and Soderman (1987). The
 394 reasons for this are not clear but it may be related to the nature of the Limit
 395 Analysis approach. The results presented are strictly only valid within this
 396 framework which essentially assumes that the soil and reinforcement are rigid-
 397 plastic materials. At failure the material must either have not yielded or if it has
 398 yielded, it must display a fully ductile plastic response with constant resistance
 399 at any strain level.

400 In practice many geotextiles do display this type of response and so it would
 401 be reasonable to assume that soil and geotextile can reach full strength at com-
 402 patible strain levels at failure. It would be necessary to check that the the limit
 403 analysis results indicate reasonably uniform elongation rates along the length of
 404 the failing zone, so that high concentrations of strain are not anticipated.

405 For geotextiles that would rupture rather than stretch at a relatively low
 406 strain level, then their (suitably factored) strength should be chosen to be

407 greater than the limiting value R_L . For such cases it is observed that the
408 interface coefficients α_c and α_s do influence the results (by $\sim 10\%$), whereas
409 below this value the reinforcement will tend to yield before the shear strength
410 on the interface is reached, thus rendering the value of α less significant (as long
411 as it is reasonably large).

412 8. Conclusions

- 413 1. The DLO analysis has been shown to find more critical failure mecha-
414 nisms compared with other limit equilibrium results in the literature for
415 most cases. It was also able to identify a previously unreported bearing
416 type failure mechanism which involves rotational ‘snapping’ of the em-
417 bankment.
- 418 2. The use of reinforcement allows an embankment of a given height H to
419 be constructed on a depth D of soft soil of around 50-100% the strength
420 of that on which an unreinforced embankment could be constructed, de-
421 pending on the value of H/D . Use of very strong compared to lower
422 strength embankment fill has only a marginal additional effect of allowing
423 construction on a soft soil of around 10% lower strength.
- 424 3. Design charts have been presented that can be used for determining the
425 maximum stable height and required reinforcement strength for fully re-
426 inforced (where the reinforcement is not taken to yield) and unreinforced
427 embankments resting over soft soil and the transition between these two
428 states which is shown to result in an approximately linear relationship
429 between the required reinforcement rupture strength and the undrained
430 shear strength of the soft soil.
- 431 4. It is recommended that embankments be designed at the point where the
432 reinforcement is not taken to yield to avoid an observed sensitivity to the
433 soft soil strength for cases where reinforcement and soil yield together.

435 Appendix

436 Appendix A. Precision of DLO solution

437 Figure A.1 shows the factor of safety on soil strength versus the number of nodes across embankment height. A value of 5 nodes across the embankment
 438 height provides an accuracy of 1-2%.

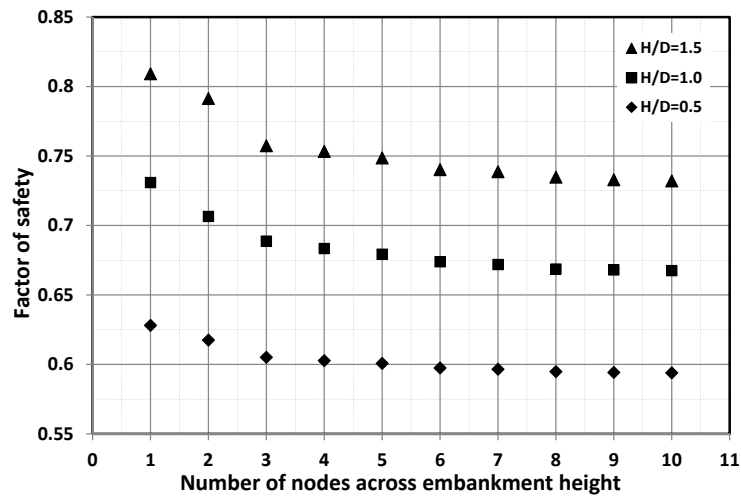


Figure A.1: Variation of factor of safety versus DLO nodal spacing

440 **References**

- 441 Chai, J.C., Bergado, D., 1993. Some techniques for finite element analysis of
442 embankments on soft ground. *Canadian Geotechnical Journal* 30, 710–719.
- 443 Clarke, S., Smith, C., Gilbert, M., 2013. Modelling discrete soil reinforcement
444 in numerical limit analysis. *Canadian Geotechnical Journal* 50, 705–715.
- 445 Duncan, J., 1996. State of the art: Limit equilibrium and finite-element analysis
446 of slopes. *Journal of Geotechnical Engineering* 122, 557–596.
- 447 Duncan, J.M., Buchignani, A.L., De Wet, M., 1987. An engineering manual
448 for slope. Virginia Polytechnic Institute and State University Reproduced
449 by the University of Wisconsin-Madison with permission and courtesy of the
450 Virginia Polytechnic Institute and State University.
- 451 Duncan, J.M., Schaefer, V.R., 1988. Finite element consolidation analysis of
452 embankments. *Computers and Geotechnics* 6, 77–93.
- 453 FHWA-NHI-00-043, 2001. Mechanically stabilized earth walls and reinforced soil
454 slopes, Design & Construction Guidelines. U.S. Department of Transportation
455 Federal Highway Administration.
- 456 Gilbert, M., Smith, C., Haslam, I., Pritchard, T., 2010. Application of disconti-
457 nuity layout optimization to geotechnical engineering, pp. 169–174. Proceed-
458 ings of the 7th European Conference on Numerical Methods in Geotechnical
459 Engineering.
- 460 Hird, C.C., 1986. Stability charts for reinforced embankment on soft ground.
461 *Geotextiles and Geomembranes* 4, 107–127.
- 462 Hird, C.C., Kwok, C.M., 1989. Finite element studies of interface behaviour
463 in reinforced embankments of soft ground. *Computers and Geotechnics* 8,
464 111–131.
- 465 Hird, C.C., Pyrah, I.C., Russell, D., 1990. Finite element analysis of the collapse
466 of reinforced embankments on soft ground. *Geotechnique* 40, 633–640.
- 467 Jewell, R.A., 1988. The mechanics of reinforced embankment on soft soils.
468 *Geotextiles and Geomembranes* 7, 237–273.
- 469 Jewell, R.A., 1996. Soil reinforcement with geotextile. London: Construction
470 Industry Research and Information Association.
- 471 Leshchinsky, B., 2015. Bearing capacity of footings placed adjacent to c' -
472 ϕ' slopes. *Journal of Geotechnical and Geoenvironmental Engineering* 141,
473 04015022.
- 474 Leshchinsky, D., 1987. Short-term stability of reinforced embankment over
475 clayey. *Soil and Foundation* 29, 105–114.

- 476 Leshchinsky, D., Smith, D.S., 1989. Deep seated failure of a granular embankment over clay: Stability analysis. *Soil and Foundation* 27, 43–57.
- 478 Leshchinsky, D., Vahedifard, F., Leshchinsky, B.A., 2012. Revisiting bearing capacity analysis of MSE walls. *Geotextiles and Geomembranes* 34, 100–107.
- 480 LimitState, 2014. *LimitState:GEO Manual Version 3.2.a.* june 2014 ed. LimitState Ltd.
- 482 Manceau, S., Macdiarmid, C., Horgan, G., 2012. Design of soil reinforced slopes and structures, in: Burland, J., Chapman, T., Skinner, H., Brown, M. (Eds.), *ICE manual of geotechnical engineering, Volume II geotechnical design, Construction and verification.*, pp. 1093–1107.
- 486 Rowe, R., Li, A.L., 2005. Geosynthetic-reinforced embankments over soft foundation. *Geosynthetics International* 12, 50–85.
- 488 Rowe, R.K., Hinchberger, S.D., 1998. The significance of rate effects in modelling the sackville test embankment. *Canadian Geotechnical Journal* 35, 500–516.
- 491 Rowe, R.K., Li, A.L., 1999. Reinforced embankment over soft foundations under undrained and partially drained conditions. *Geotextiles and Geomembranes* 17, 129–146.
- 494 Rowe, R.K., Soderman, K., 1987. Stabilization of very soft soils using high strength geosynthetics: the role of finite element analyses. *Geotextiles and Geomembranes* 6, 53–80.
- 497 Rowe, R.K., Soderman, K.L., 1985. An approximate method for estimating the stability of geotextile-reinforced. *Canadian Geotechnical Journal* 22, 392–398.
- 499 Sabhahit, N., Basudhar, P.K., Madhav, M.R., Miura, N., 1994. Generalized stability analysis of reinforced embankment on soft clay. *Geotextiles and Geomembranes* 13, 765–780.
- 502 Smith, C., Gilbert, M., 2007. Application of discontinuity layout optimization to plane plasticity problems. *Royal Society A: Mathematical, Physical and Engineering Sciences* 463, 2461–2484.
- 505 Smith, C.C., Gilbert, M., 2013. Identification of rotational failure mechanisms in cohesive media using discontinuity layout optimisation. *Geotechnique* 63, 1194–1208.
- 508 Tandjiria, V., Low, B.K., Teh, C.I., 2002. Effect of reinforcement force distribution on stability of embankments. *Geotextiles and Geomembranes* 20, 423–443.
- 511 Vahedifard, F., Leshchinsky, B.A., Sehat, S., Leshchinsky, D., 2014. Impact of cohesion on seismic design of geosynthetic-reinforced earth structures. *Journal of Geotechnical and Geoenvironmental Engineering* 140, 04014016.

514 Zhang, N., Shen, S.L., Wu, H.N., Chai, J.C., Xu, Y.S., Yin, Z.Y., 2015. Evalua-
515 tion of effect of basal geotextile reinforcement under embankment loading on
516 soft marine deposits. *Geotextiles and Geomembranes* 43, 506 – 514. Special
517 issue on Soft Ground Improvement using Geosynthetics Applications.